

RESEARCH

Open Access



# Nontargeted metabolomics reveals the potential mechanism underlying the association between birthweight and metabolic disturbances

Xiao Zhai<sup>1†</sup>, Jieying Liu<sup>1,2†</sup>, Miao Yu<sup>1</sup>, Qian Zhang<sup>1</sup>, Ming Li<sup>1</sup>, Nan Zhao<sup>2</sup>, Juntao Liu<sup>3</sup>, Yingna Song<sup>3</sup>, Liangkun Ma<sup>3</sup>, Rongrong Li<sup>4</sup>, Zongxu Qiao<sup>5</sup>, Guifen Zhao<sup>5</sup>, Ruiping Wang<sup>5</sup> and Xinhua Xiao<sup>1\*</sup>

## Abstract

**Aims** The aim of this study was to characterize the metabolites associated with small- and large-gestational-age newborns in maternal and cord blood, and to investigate potential mechanisms underlying the association between birthweight and metabolic disturbances.

**Research design and methods** We recorded detailed anthropometric data of mother-offspring dyads. Untargeted metabolomic assays were performed on 67 pairs of cord blood and maternal fasting plasma samples including 16 pairs of small-for-gestational (SGA, < 10th percentile) dyads, 28 pairs of appropriate-for-gestational (AGA, approximate 50 percentile) dyads, and 23 pairs of large-for-gestational (LGA, > 90th percentile) dyads. The association of metabolites with newborn birthweight was conducted to screen for metabolites with U-shaped and line-shaped distributions. The association of metabolites with maternal and fetal phenotypes was also performed.

**Results** We found 2 types of metabolites that changed in different patterns according to newborn birthweight. One type of metabolite exhibited a “U-shaped” trend of abundance fluctuation in the SGA-AGA-LGA groups. The results demonstrated that cuminaldehyde level was lower in the SGA and LGA groups, and its abundance in cord blood was negatively correlated with maternal BMI ( $r = -0.352$ ,  $p = 0.009$ ) and weight gain ( $r = -0.267$ ,  $p = 0.043$ ). 2-Methoxy-estradiol-17b 3-glucuronide, which showed enrichment in the SGA and LGA groups, was positively correlated with homocysteine ( $r = 0.44$ ,  $p < 0.001$ ) and free fatty acid ( $r = 0.42$ ,  $p < 0.001$ ) in maternal blood. Serotonin and 13(S)-HODE were the second type of metabolites, denoted as “line-shaped”, which both showed increasing trends in the SGA-AGA-LGA groups in both maternal and cord blood and were both significantly positively correlated with maternal BMI before pregnancy. Moreover, cuminaldehyde, serotonin, 13(S)-HODE and some lipid metabolites showed a strong correlation between maternal and cord blood.

**Conclusions** These investigations demonstrate broad-scale metabolomic differences associated with newborn birthweight in both pregnant women and their newborns. The U-shaped metabolites associated with both the SGA and LGA groups might explain the U-shaped association between birthweight and metabolic dysregulation.

<sup>†</sup>Xiao Zhai and Jieying Liu share first authorship.

\*Correspondence:

Xinhua Xiao

xiaoxh2014@vip.163.com

Full list of author information is available at the end of the article



© The Author(s) 2023. **Open Access** This article is licensed under a Creative Commons Attribution 4.0 International License, which permits use, sharing, adaptation, distribution and reproduction in any medium or format, as long as you give appropriate credit to the original author(s) and the source, provide a link to the Creative Commons licence, and indicate if changes were made. The images or other third party material in this article are included in the article's Creative Commons licence, unless indicated otherwise in a credit line to the material. If material is not included in the article's Creative Commons licence and your intended use is not permitted by statutory regulation or exceeds the permitted use, you will need to obtain permission directly from the copyright holder. To view a copy of this licence, visit <http://creativecommons.org/licenses/by/4.0/>. The Creative Commons Public Domain Dedication waiver (<http://creativecommons.org/publicdomain/zero/1.0/>) applies to the data made available in this article, unless otherwise stated in a credit line to the data.

The line-shaped metabolites might participate in intrauterine growth regulation. These observations might help to provide new insights into the insulin resistance and the risk of metabolic disturbance of SGA and LGA babies in adulthood and might identify potential new markers for adverse newborn outcomes in pregnant women.

**Keywords** Metabolomics, Newborn birthweight, Metabolic disturbances

## Introduction

Disturbances in fetal growth could greatly increase the susceptibility to chronic metabolic diseases in adulthood, mainly obesity, insulin resistance, impaired glucose tolerance, dyslipidemia, and cardiovascular diseases [1–3]. It has been recognized for years that small-for-gestational-age (SGA) infants are associated with a high risk of developing metabolic dysregulations in adulthood [3–7]. In addition, infants born as large-for-gestational-age (LGA) are also at a higher risk of T2DM and obesity [8]. This demonstrates the U-shaped relationship between birthweight and the risk of T2DM [9]. The hypothesis of “fetal origins of adult diseases” proposed by Barker et al. indicates that intrauterine factors have long-term programming effects on fetal development and lead to increased vulnerability to chronic diseases later in life, often in adulthood [1]. This concept was initially supported by studies on children with SGA [10] and maternal malnutrition [11] associated with increased susceptibility to chronic diseases later in life. Studies on prenatal famine during the Dutch Hunger Winter [12] and adults born during the Chinese famine between 1959 and 1961 [13] found that individuals who were exposed to famine in utero were more prone to be overweight and have T2DM. The thrifty phenotype attributes the relationship of adverse intrauterine growth and subsequent increased metabolic risk to the compensatory response to undernutrition status in early life, leading to permanent changes in metabolism [1].

While the foundational studies of this “fetal origins of adult diseases” theory focused on the influence of prenatal undernutrition on offspring, an increasing body of studies have focused on the impact of maternal obesity and diabetes during pregnancy on offspring. Evidence has shown that maternal obesity and overnutrition are linked to a higher incidence of macrosomia or LGA and have a potential impact on future metabolic risk [2, 14, 15]. For instance, maternal prepregnancy obesity and excessive gestational weight gain are associated with higher offspring birthweight and childhood adiposity [16]. Moreover, a positive association has been discovered between maternal diabetes or third-trimester glucose tolerance with higher offspring birth weight and youth-onset T2DM incidence [17].

However, the mechanism underlying the association between high or low birthweight and T2DM risk remains

unclear. It is quite interesting that high- and low-birthweight infants are likely exposed to different intrauterine environments; yet, they both have an elevated tendency to develop metabolic diseases in adulthood. Therefore, we hypothesized that high- and low-birthweight infants could share similar metabolic alterations reflecting underlying important biomolecular mechanisms linked to these processes.

There is an urgent need to understand the complex intrauterine biomolecular perturbations and to identify individuals at risk of metabolic disturbances. Since the exchange of nutrients for fetal metabolism by the placenta is essential for fetal growth and due to the placental barrier, most substances that pass through the barrier are small and hydrophobic molecules, such as glucose, amino acids and fatty acids [18]. The analysis of the metabolite profile in maternal blood and fetal cord blood might reflect parts of the material exchange and depict the intrauterine environment at a glance. Consequently, using rapidly developing metabolomics technologies that focus on the quantity of low molecular weight (< 1500 Da) metabolites offers an integrative perspective into this maternal–fetal metabolism status. Full-scan nontargeted Q-TOF coupled with liquid chromatography can provide excellent robustness, and hundreds of samples can be profiled [19].

In this study, we aimed to characterize the metabolic phenotypes of pregnant women and their newborn babies with high or low birth weight, identify metabolic perturbations linked to birth weight, and explore potential biomolecular mechanisms linked to abnormal birth weight.

## Research design and methods

### Data and sample collection

This study recruited mother–offspring dyads from the outpatient clinic and/or the delivery ward of the Department of Obstetrics and Gynecology at Peking Union Medical College Hospital (PUMCH) and Xingtai People's Hospital (XTPH) in China from September 2017 to July 2018. The inclusion criteria were as follows: being singleton pregnant, maternal age between 18 and 45, and gestational age (GA) between 37 and 42 weeks. Participants who had smoked or had alcohol use during pregnancy and those who had been diagnosed with hypertension

or preeclampsia were excluded from this study. The study protocol was approved by the ethics committees of PUMCH and the ethics committee of XTRH, and written informed consent was obtained from all participants prior to recruitment.

A total of 165 mother–offspring dyads were admitted to our study. According to the birth weight of neonates and the Chinese neonatal birth weight report [20], the birth weight of neonates are classified as SGA (<10th percentile), appropriate for gestational (AGA) (approximately 50th percentile), and LGA (>90th percentile) based on gestational age. 16 pairs of SGA dyads, 28 pairs of AGA dyads, and 23 pairs of LGA dyads were selected for this study. Participating mothers underwent a 75-g oral glucose tolerance test (OGTT) between 24 and 28 weeks of gestation. Maternal anthropometric measurements, including height, weight, and mean arterial pressure, were measured by doctors. Information on maternal age, parity, past medical history, prepregnancy weight, and gestational weight gain were collected from their pregnancy health records. Prepregnancy body mass index (BMI) was calculated as prepregnancy weight in kilograms divided by measured height in meters squared ( $\text{kg}/\text{m}^2$ ). Birth weight, newborn sex, mode of delivery, and gestational age were obtained from the hospital delivery records.

Maternal blood samples were collected in a fasting state between 37 and 42 weeks gestational age during routine blood sampling from the outpatient clinic. Cord vein blood samples were obtained within 10 min of delivery. The blood samples were collected into 2-ml EDTA containers and placed on ice. The blood was immediately centrifuged (3000 rpm, 15 min) at 4 °C, plasma was separated, and aliquots (0.2 ml) were rapidly stored at -80 °C until metabolomic assays.

### Conventional metabolite analysis

Conventional metabolites were measured on a Beckman Coulter AU5800. Hypersensitive C-reactive protein (hs-CRP), C-peptide (C-Pep) and insulin were measured using reagents from Beckman (Brea, CA). Glucose, triglycerides (TGs), total cholesterol (TC), high-density lipoprotein cholesterol (HDL-C), low-density lipoprotein cholesterol (LDL-C), lipoprotein(a) (Lp(a)) and free fatty acids (FFAs) were measured using reagents from Sekisui (Tokyo, JPN). Additionally, homocysteine (HCY) was measured using reagents from Leadman (Beijing, CHN), and glycated albumin (GA) was measured using reagents from Asahi (Tokyo, JPN). Leptin and adiponectin were analyzed by an enzyme-linked immunosorbent assay (Crystal Chemistry, IL, USA).

### Nontargeted metabolomics assays

The nontargeted metabolomics assays were conducted as previously reported [19]. Specifically, a system coupling ultraperformance liquid chromatography (UPLC, Waters ACQUITY UPLC I-Class) to time-of-flight (TOF, Waters XevoG2-XS Qtof) mass spectrometry was used to analyze the full range of metabolites present in plasma. Methanol at a ratio of 3:1 (vol/vol) to the sample was added for protein removal overnight at -20 °C. The samples were centrifuged, and the supernatants were analyzed directly. Quality control (QC) pools were constructed using equal volumes from all the samples, prepared for analysis as described above, and injected every 10 samples for all the runs. The mass spectrometers (MSs) adopted both positive and negative ionization modes, which helped detect more compounds. Progenesis QI software (Waters) performs peak picking and drift alignment (retention time and accurate mass) based on QC samples [17]. The annotation of metabolites was in Progenesis QI, the spectra are matched against reference spectra in HMDB (<http://www.hmdb.ca/>), METLIN and KEGG databases [21].

### Statistical analyses

#### Conventional metabolites and group comparisons

All statistical analyses were performed in SPSS version 25.0 (SPSS, Chicago, IL). Means and SDs of conventional metabolites were calculated. Categorical variable frequencies and continuous variable means were compared between 3 groups using Fisher's exact tests and one-way ANOVA, respectively.

#### Nontargeted metabolomic analysis

As previously reported [22], multivariate analysis was conducted using partial least squares regression discriminant analysis (PLS-DA) in SGA/AGA/LGA group comparisons in SIMCA version 14.1 (MKS Umetrics AB, Umea, Sweden). Orthogonal partial least squares regression discriminant analysis (OPLS-DA) was used in SGA/AGA and AGA/LGA maternal and fetal comparisons. Three parameters, including  $R^2$  and  $Q^2$ , were used to evaluate the quality and reliability of these models. Individual metabolites were selected based on the variable importance in projection (VIP), and metabolites in which  $\text{VIP} > 1$  were selected and processed for the following meta-analysis.

The peak intensity data, which represent the metabolite abundance in each sample, were normalized using Z score transformation for meta-analysis. We first identified the overlapping metabolites between the maternal and fetal groups in a Venn diagram using the R package VennDiagram and selected the metabolites with

the same change direction presented in the heatmap using the R package ComplexHeatmap. In this study, 2 types of metabolites were separately analyzed, including U-shaped (higher or lower in both the SGA/LGA group) and line-shaped (the abundance in the SGA/AGA/LGA group trend according to the birthweight of offspring). MetaboAnalyst 5.0 (<https://www.metaboanalyst.ca/>) was used for metabolomic pathway analysis [23].

### Statistical-analysis

Continuous variables were described as the means with SD. Categorical variables are represented as frequencies with proportions. The correlation of the maternal and fetal metabolome was calculated and drawn using the

Spearman method by the R package “ggplot2”. Spearman’s correlation analysis was used to assay the correlation between metabolites and clinical parameters, as for model 1. For model 2, Partial correlation coefficients were calculated to evaluate the association between metabolites and clinical parameters after adjusting for confounders. *r* coefficient was calculated after adjusting for maternal age, parity and gestational age, and fetal sex. A *P* value < 0.05 (two-sided) was considered statistically significant.

## Results

### Population characteristics

The following 67 pairs of mother–offspring dyads were included in this study: 16 pairs of SGA (< 10th percentile)

**Table 1** Demographics of mothers and their offspring

Characteristic	SGA	AGA	LGA	<i>P</i>
<b><i>N</i></b>	16	28	23	
<b>Field center, <i>N</i> (%)</b>				
PUMCH, Beijing	6 (37.5)	11 (39.3)	7 (30.4)	0.81
XTPH, Hebei	10 (62.5)	17 (60.7)	16 (69.6)	
<b>Maternal parity, <i>N</i> (%)</b>				
First child	11 (68.8)	8 (28.6)	14 (60.9)	<b>0.02</b>
Subsequent child	5 (31.2)	20 (71.4)	9 (39.1)	
<b>New born sex, <i>N</i> (%)</b>				
Male	12 (75.0)	15 (53.6)	14 (60.9)	0.41
Female	4 (25.0)	13 (46.4)	9 (39.1)	
<b>Mode of delivery, <i>N</i> (%)</b>				
Vaginal	7 (43.8)	10 (35.7)	3 (13.0)	0.08
Cesarean section	9 (56.2)	18 (64.3)	20 (87.0)	
<b>Maternal Characteristics, Mean (SD)</b>				
Maternal age (years)	31.4 (4.6)	33.7 (6.7)	30.9 (5.3)	0.20
Gestational age (weeks)	38.7 (1.1)	38.4 (0.9)	39.0 (1.1)	0.13
Prepregnancy BMI (kg/m <sup>2</sup> )	22.4 (3.4)	23.4 (3.5)	25.1 (2.6)	<b>0.03</b>
Gestational weight gain(kg)	14.8 (5.2)	14.2 (6.0)	15.5 (5.8)	0.74
Mean arterial pressure(mmHg)	89.5 (10.2)	89.2 (9.2)	89.6 (9.7)	0.94
Maternal GDM, <i>N</i> (%)	8 (50.0)	18 (64.3)	13 (56.5)	0.67
Fasting plasma glucose(mmol/L)	4.6 (0.7)	4.7 (0.6)	4.6 (0.5)	0.78
Fasting C-peptide (ng/mL)	2.7 (2.3)	2.2 (0.6)	2.3 (0.7)	0.37
Fasting Insulin (μU/mL)	10.7 (6.8)	11.8 (3.8)	13.7 (5.6)	0.27
Leptin (ng/mL)	644.9 (494.1)	413.5 (311.1)	518.5 (391.8)	0.17
Adiponectin (ng/mL)	6135.8 (3230.1)	6908.0 (5258.9)	6641.8 (393.2)	0.88
<b>Newborn Characteristics, Mean (SD)</b>				
Birthweight(g)	2739.4 (250.7)	3300.4 (133.2)	4097.0 (238.2)	<b>&lt; 0.001</b>
Cord glucose(mmol/L)	4.4 (1.3)	4.5 (1.6)	4.4 (2.1)	0.98
Cord C-peptide (ng/mL)	0.6 (0.2)	1.1 (1.3)	1.4 (0.9)	0.08
Cord Insulin (μU/mL)	4.2 (2.2)	6.9 (3.9)	14.9 (21.1)	<b>0.04</b>
Cord Leptin (ng/mL)	43.7 (42.8)	118.7 (203.5)	355.6 (531.5)	<b>0.02</b>
Cord Adiponectin (ng/mL)	26,221.2 (8062.6)	27,014.2(10,613.8)	28,995.6 (9760.0)	0.72

Data are *n* (%) or means ± SD unless otherwise indicated. Categorical variable frequencies and continuous variable means were compared for SGA/AGA/LGA mothers using Fisher’s exact tests and one-way ANOVA, respectively

dyads, 28 pairs of AGA dyads (approximately 50th percentile), and 23 pairs of LGA (>90th percentile) (Table 1). Most of the clinical characteristics were similar among the 3 groups. Maternal age, gestational age, maternal GDM proportion and most clinical biochemical indices, including fasting plasma glucose, insulin, FFA, TC, TG, leptin and adiponectin, showed no significant difference between SGA, AGA and LGA mothers. The prepregnancy BMIs were 22.4, 23.4 and 25.1 in the SGA, AGA and LGA groups, respectively ( $p=0.03$ ). Moreover, HDL-C in LGA mothers (Supplemental Table S1) was significantly lower than that in the other two groups ( $p=0.01$ ). Regarding newborn characteristics, cord blood insulin ( $p=0.04$ ) and leptin ( $p=0.02$ ) were significantly higher in the LGA group.

### Metabolomic analysis

Supervised PLS-DA analysis was performed to investigate the metabolite profiles of each group, obtaining improved and better discrimination (Fig. 1). The metabolites that contributed to the separation of the SGA and AGA groups in the mother and their offspring were selected by the VIP value (>1) calculated from the OPLS-DA model (Figure S1 and S2, Table S4), as well as those metabolites for the LGA and AGA comparison.  $R^2$  and  $Q^2$  values for SGA vs AGA maternal metabolome are 0.857 and -0.569 (Negative mass mode), 0.943 and -0.119 (Positive mass mode).  $R^2$  and  $Q^2$  values for SGA vs AGA fetal metabolome are 0.958 and 0.0121 (Neg), 0.921 and -0.57 (Pos).  $R^2$  and  $Q^2$  values for LGA vs AGA

maternal metabolome are 0.955 and 0.155 (Neg), 0.959 and -0.104 (Pos).  $R^2$  and  $Q^2$  values for LGA vs AGA fetal metabolome are 0.944 and 0.0407 (Neg), 0.887 and -0.361 (Pos).

From the Venn diagram (Fig. 2), we identified 1518 and 1456 metabolites that contributed to the separation of LGA versus AGA mothers and their offspring (differential metabolites, DMs), respectively, and mothers and their offspring shared 827 DMs. Meanwhile, there were 1371 and 1383 metabolites that attribute to the separation of SGA versus AGA mother and offspring, respectively, and mothers and their offspring share 663 DMs. Overlapping of these 4 kinds of DMs yielded 257 metabolites that represent the same DMs shared by both the SGA and LGA groups when compared with the AGA group.

Among these 257 metabolites (MS details are shown in Supplementary Table S4), we identified 2 types of metabolites from the heatmap (Fig. 3A), including 33 “line-shaped” metabolites (Fig. 3B) and 44 “U-shaped” metabolites (Fig. 3C). The fold change between SGA and AGA, or LGA and AGA was calculated (Table S4), and the U-shaped metabolites were higher or lower in both SGA/LGA mothers and babies (means fold change of SGA/AGA and LGA/AGA are both >1 or <1), while line-shaped metabolites were increased or decreased among SGA/AGA/LGA mothers and babies (means fold change of SGA/AGA >1 and LGA/AGA <1, or fold change of SGA/AGA <1 and LGA/AGA >1)..

We put 33 line-shaped and 44 U-shaped metabolites into pathway analysis, respectively. The topological

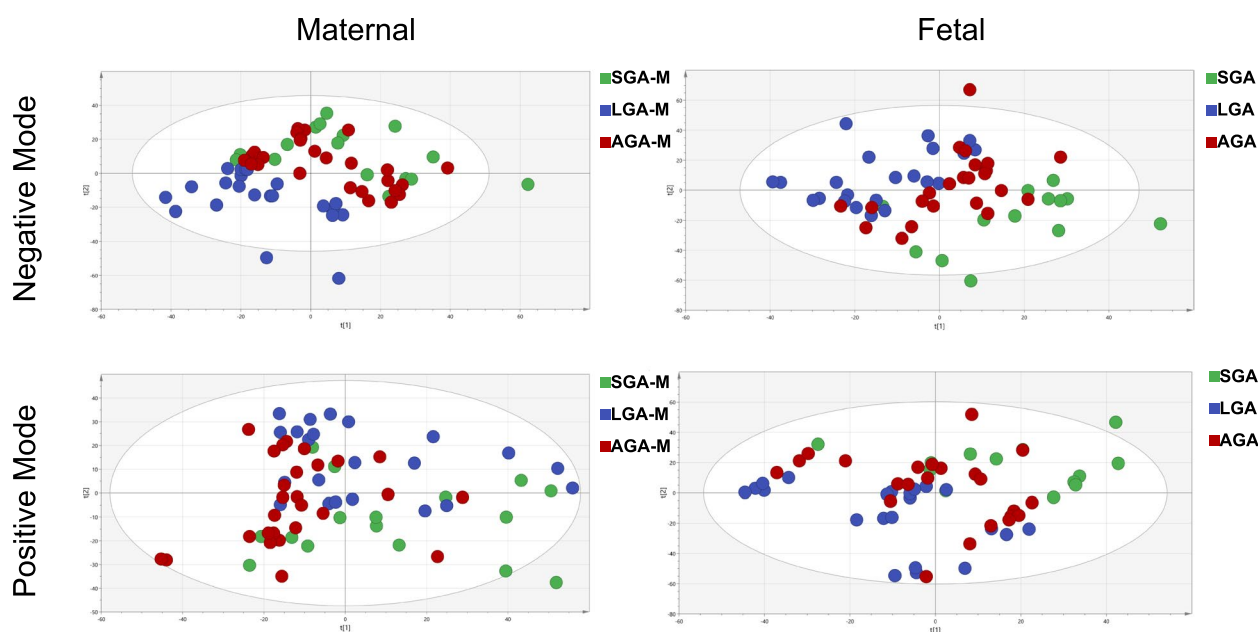


**Fig. 1** PLS-DA score plot for maternal and fetal metabolome under negative and positive MS mode



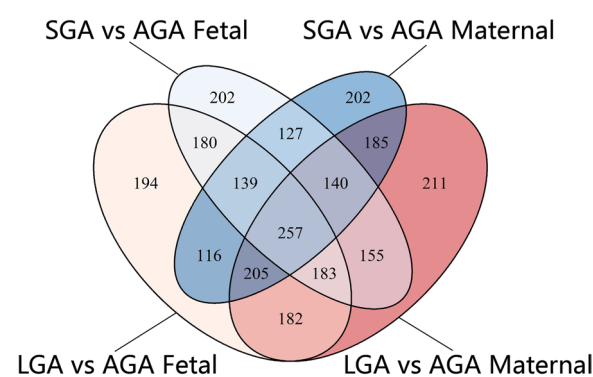


**Fig. 2** Venn diagram showing the identified metabolites selected by the OPLS-DA models

impact factors and enrichment analysis p-values of the corresponding pathways are shown in the bubble graph (Fig. S1). The results suggested that U-shaped metabolites were enriched in linoleic acid metabolism (metabolites including Phosphatidylcholine-PC), arachidonic acid metabolism (metabolites including PC, Prostaglandin E2), and glycerophospholipid metabolism (metabolites including PC, Citicoline)

(Fig. S3A). Line-shaped metabolites were enriched in glycerophospholipid metabolism (metabolites including phosphatidylethanolamine-PE, PC, 1-Acyl-sn-glycero-3-phosphocholine-LysoPC), alpha-linolenic acid metabolism (metabolites including PC, tetracosanoic acid, 13(S)-HODE), and linoleic acid metabolism (metabolites including PC) (Fig. S3B).

### Metabolites associated with newborn birthweight

As shown in Fig. 4A, the U-shaped metabolites were more highly expressed in both SGA and LGA maternal and cord blood, including L-carnitine, PG(16:1/ 22:6) (denoted PG) and 2-methoxy-estradiol-17b 3-glucuronide (denoted glucuronide). However, cuminaldehyde was significantly downregulated in the SGA and LGA groups.

As shown in Fig. 4B, line-shaped metabolites, including serotonin, 13S-hydroxyoctadecadienoic acid (denoted as 13(S)-HODE) and MG(0:0/24:6/0:0) (denoted as MG), showed increasing trends in both mothers and babies among the SGA, AGA and LGA groups. LysoPC(p-18:1/0:0) (denoted as LysoPC) showed decreasing trends in both mothers and babies among the SGA, AGA and LGA groups.

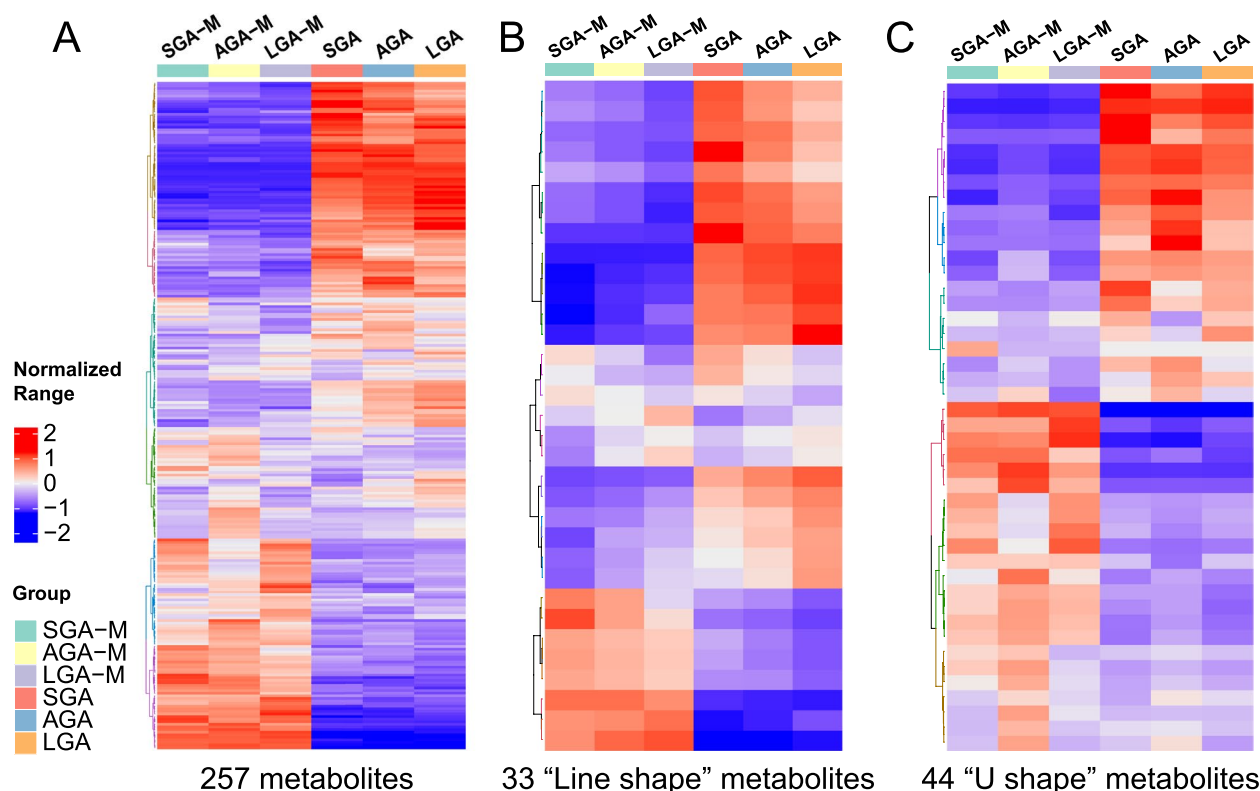


**Fig. 3** Heatmap showing normalized metabolite abundance in different groups. **A** The 257 metabolites shared by the SGA and LGA groups and different from the AGA group; **B** The 33 line-shaped metabolites display the increasing/decreasing abundance in the SGA/AGA/LGA group according to the newborn birthweight. **C** The 44 U-shaped metabolites display higher or lower abundance in both the SGA and LGA groups

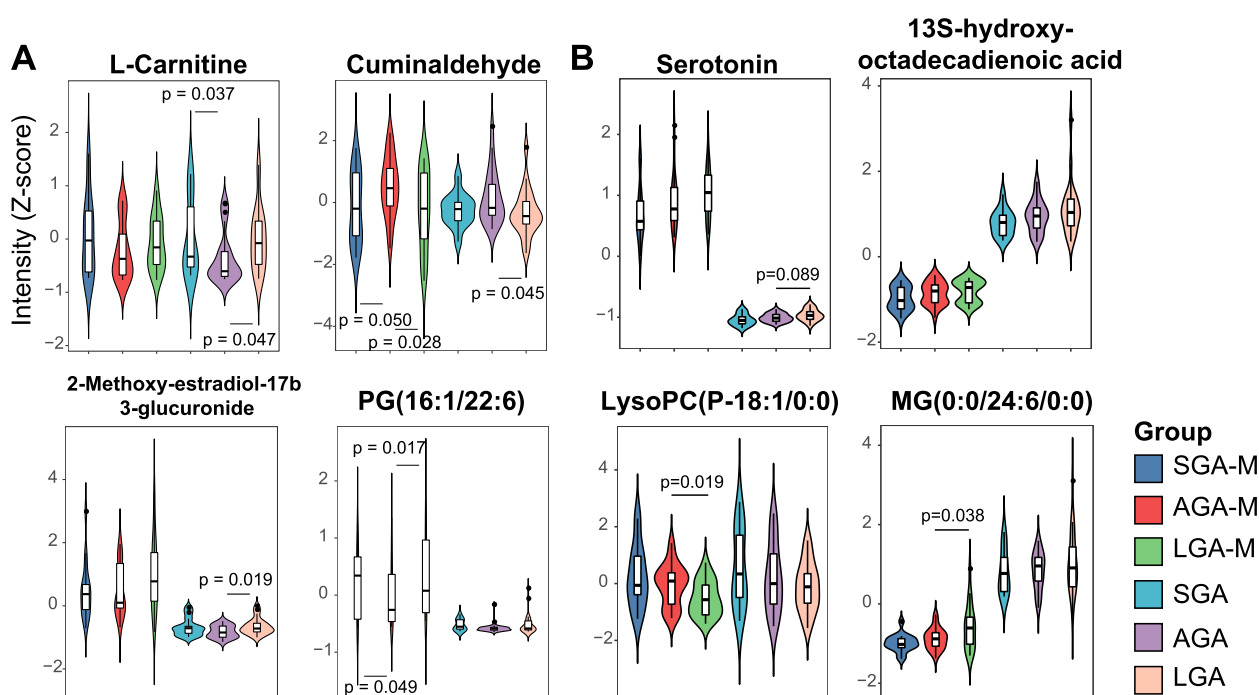


**Fig. 4** Abundance of metabolites in different groups. **A** Representative U-shapes metabolites; **B** Representative line-shaped metabolites; Abundance was normalized using Z score transformation of intensity

#### Correlation between maternal and fetal metabolite abundance

The correlation between the maternal and fetal metabolome was analyzed using the Spearman method (Fig. 5). Among U-shaped metabolites, L-carnitine ( $r = 0.72$ ,  $p < 0.001$ ), cuminaldehyde ( $r = 0.38$ ,  $p = 0.004$ ) and PG ( $r = 0.31$ ,  $p = 0.02$ ) in maternal and cord blood were significantly positively correlated. Among line-shaped metabolites, serotonin ( $r = 0.32$ ,  $p < 0.001$ ), 13(S)-HODE ( $r = 0.54$ ,  $p < 0.001$ ), LysoPC ( $r = 0.42$ ,  $p = 0.001$ ), and monoacylglyceride ( $r = 0.42$ ,  $p = 0.001$ ) in maternal and cord blood were significantly positively correlated.

#### Correlation between metabolite levels and clinical characteristics

To further investigate the association between the metabolome and clinical characteristics, partial correlation analysis was performed (Table 2 and Table 3). Among the U-shaped metabolites, cuminaldehyde was expressed at low levels in the SGA and LGA groups, and its abundance in maternal blood was positively correlated with maternal adiponectin ( $r = 0.320$ ,  $p = 0.010$ ) and HDL-C (adjusted  $r = 0.323$ ,  $p = 0.011$ ). Cuminaldehyde in cord blood was negatively correlated with maternal prepregnancy BMI (adjusted  $r = -0.356$ ,  $p = 0.009$ ) and weight gain ( $r = -0.267$ ,  $p = 0.043$ ), as shown in Table S2. L-Carnitine, PG and glucuronide were higher in the SGA and LGA groups. Maternal

glucuronide was positively correlated with maternal HCY (adjusted  $r = 0.396$ ,  $p = 0.002$ ) and FFA (adjusted  $r = 0.479$ ,  $p < 0.001$ ). Maternal glucuronide was negatively correlated with FBG (adjusted  $r = -0.360$ ,  $p = 0.005$ ) and HDL-C (adjusted  $r = -0.247$ ,  $p = 0.058$ ). Maternal PG was positively correlated with prepregnancy BMI (adjusted  $r = 0.328$ ,  $p = 0.011$ ). Cord blood PG was positively correlated with FFA (adjusted  $r = 0.285$ ,  $p = 0.045$ ).

Among the line-shaped metabolites, serotonin, 13(S)-HODE and MG showed increasing trends in the SGA, AGA and LGA groups. The abundance of serotonin in maternal blood was significantly positively correlated with prepregnancy BMI ( $r = 0.259$ ,  $p = 0.037$ ) and maternal HCY ( $r = 0.361$ ,  $p = 0.003$ ). Cord blood serotonin levels were also significantly positively correlated with prepregnancy BMI (adjusted  $r = 0.354$ ,  $p = 0.009$ ) and cord blood glucose ( $r = -0.355$ ,  $p = 0.008$ ). Maternal 13(S)-HODE was positively correlated with maternal prepregnancy BMI (adjusted  $r = 0.441$ ,  $p < 0.001$ ), weight gain (adjusted  $r = 0.400$ ,  $p = 0.002$ ), and maternal HCY ( $r = 0.258$ ,  $p = 0.038$ ) and negatively correlated with maternal adiponectin ( $r = -0.28$ ,  $p = 0.023$ ). Moreover, maternal MG was positively related to maternal FFA (adjusted  $r = 0.315$ ,  $p = 0.014$ ). Maternal LysoPC showed decreasing trends in the SGA, AGA and LGA groups that were positively related to maternal HDL-C ( $r = 0.286$ ,  $p = 0.021$ ), as well as LysoPC in cord blood with cord HDL-C ( $r = 0.263$ ,  $p = 0.050$ ).

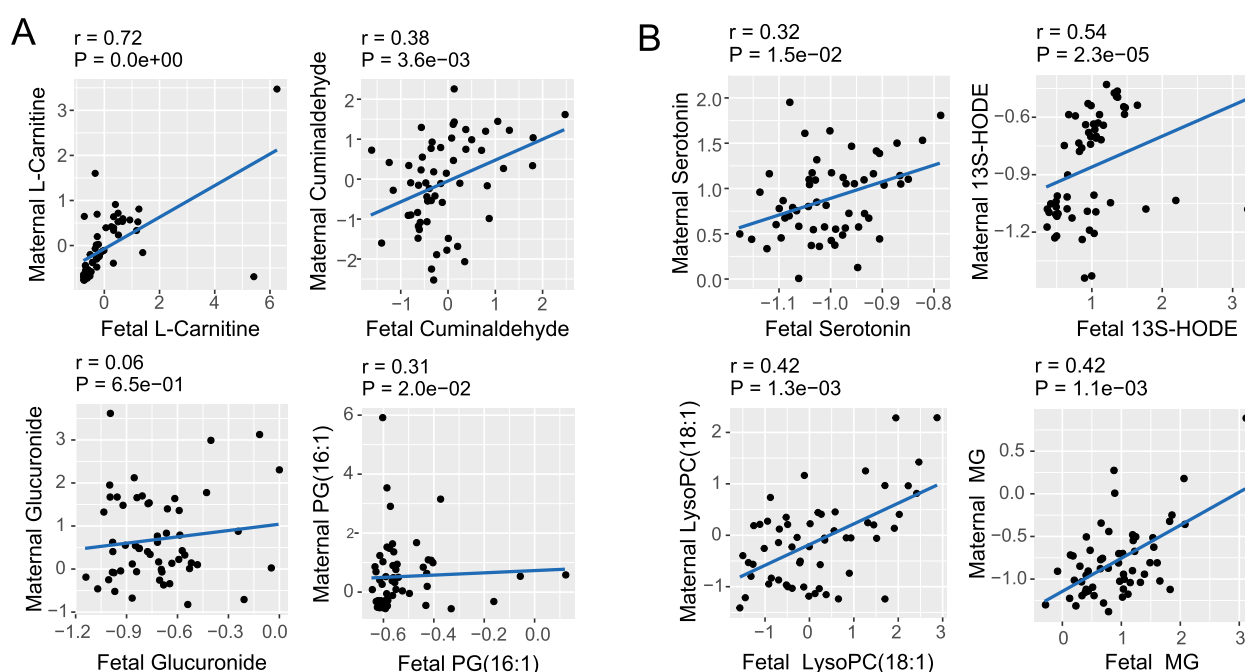


**Fig. 5** Association of metabolites in maternal and cord blood. **A** Representative U-shaped metabolites; **B** Representative line-shaped metabolites

**Table 2** Correlation of U-shaped metabolites and blood index in maternal blood

		L-Carnitine		Cuminaldehyde		2-methoxy-estradiol-17b 3-glucuronide			
		r	P	r	P	r	P	r	P
<b>BMI</b>	Model1	-0.005	0.971	-0.179	0.154	0.177	0.158	<b>0.280</b>	<b>0.024</b>
	Model2	0.017	0.899	-0.180	0.169	0.110	0.403	<b>0.328</b>	<b>0.011</b>
<b>Weight Gain</b>	Model1	-0.140	0.267	<b>-0.252</b>	<b>0.043</b>	0.146	0.245	0.224	0.073
	Model2	-0.200	0.125	-0.240	0.065	0.071	0.591	-0.099	0.452
<b>HbA1c</b>	Model1	-0.099	0.496	-0.226	0.115	0.101	0.486	-0.164	0.255
	Model2	-0.149	0.329	-0.153	0.316	-0.091	0.554	-0.075	0.625
<b>FBG</b>	Model1	0.200	0.113	0.030	0.815	<b>-0.424</b>	<b>&lt; 0.001</b>	-0.009	0.943
	Model2	0.205	0.119	0.036	0.788	<b>-0.360</b>	<b>0.005</b>	0.126	0.341
<b>HDL-C</b>	Model1	-0.064	0.610	0.242	0.052	<b>-0.254</b>	<b>0.041</b>	-0.110	0.384
	Model2	-0.026	0.845	<b>0.329</b>	<b>0.010</b>	-0.247	0.058	-0.124	0.347
<b>LDL-C</b>	Model1	0.052	0.681	0.067	0.599	-0.070	0.581	-0.204	0.103
	Model2	0.021	0.872	0.081	0.536	-0.116	0.378	<b>-0.276</b>	<b>0.033</b>
<b>FFA</b>	Model1	0.046	0.714	-0.150	0.234	<b>0.424</b>	<b>&lt; 0.001</b>	-0.196	0.118
	Model2	0.080	0.544	-0.140	0.287	<b>0.479</b>	<b>&lt; 0.001</b>	0.044	0.740
<b>Leptin</b>	Model1	0.098	0.440	-0.131	0.303	-0.165	0.192	<b>0.285</b>	<b>0.022</b>
	Model2	-0.023	0.861	-0.222	0.091	-0.254	0.052	0.051	0.702
<b>Adiponectin</b>	Model1	0.033	0.795	<b>0.320</b>	<b>0.010</b>	-0.185	0.143	-0.052	0.682
	Model2	0.076	0.567	0.064	0.628	0.006	0.962	0.052	0.696
<b>HCY</b>	Model1	-0.242	0.052	<b>-0.316</b>	<b>0.010</b>	<b>0.440</b>	<b>&lt; 0.001</b>	-0.150	0.234
	Model2	-0.226	0.082	-0.102	0.438	<b>0.396</b>	<b>0.002</b>	-0.084	0.523

Model 1 is non-adjusted

Model 2 is adjusted for maternal age, parity, GDM and gestational age, and fetal sex



**Table 3** Correlation of line-shaped metabolites and blood index in maternal blood

		Serotonin		13(S)-HODE		LysoPC(P-18:1)		MG(0:0/24:6)	
		r	P	r	P	r	P	r	P
<b>BMI</b>	Model1	<b>0.259</b>	<b>0.037</b>	<b>0.462</b>	<b>&lt;0.001</b>	-0.077	0.544	0.024	0.848
	Model2	0.193	0.140	0.441	<b>&lt;0.001</b>	-0.073	0.580	0.115	0.380
<b>Weight Gain</b>	Model1	0.191	0.128	<b>0.404</b>	<b>0.001</b>	-0.135	0.283	-0.120	0.341
	Model2	0.230	0.076	<b>0.400</b>	<b>0.002</b>	-0.133	0.312	-0.155	0.238
<b>HbA1c</b>	Model1	0.212	0.139	0.125	0.388	0.047	0.748	-0.055	0.705
	Model2	0.107	0.483	0.259	0.086	0.060	0.693	-0.084	0.583
<b>FBG</b>	Model1	-0.227	0.071	-0.157	0.216	<b>0.248</b>	<b>0.048</b>	0.073	0.567
	Model2	-0.188	0.155	-0.129	0.328	0.186	0.159	0.033	0.805
<b>HDL-C</b>	Model1	-0.190	0.129	-0.139	0.268	<b>0.286</b>	<b>0.021</b>	-0.073	0.563
	Model2	-0.236	0.069	-0.152	0.247	0.192	0.142	-0.145	0.270
<b>LDL-C</b>	Model1	-0.076	0.545	-0.152	0.228	0.166	0.185	0.118	0.350
	Model2	0.016	0.906	-0.041	0.758	0.216	0.098	0.044	0.741
<b>FFA</b>	Model1	<b>0.312</b>	<b>0.011</b>	0.069	0.583	-0.111	0.380	<b>0.313</b>	<b>0.011</b>
	Model2	0.303	0.019	0.052	0.695	-0.150	0.251	<b>0.315</b>	<b>0.014</b>
<b>Leptin</b>	Model1	-0.010	0.937	0.170	0.181	-0.084	0.511	-0.182	0.151
	Model2	-0.045	0.735	0.092	0.487	-0.013	0.920	-0.180	0.172
<b>Adiponectin</b>	Model1	-0.126	0.321	<b>-0.284</b>	<b>0.023</b>	0.097	0.445	-0.048	0.706
	Model2	0.000	0.997	-0.079	0.552	0.174	0.187	-0.018	0.893
<b>HCY</b>	Model1	<b>0.361</b>	<b>0.003</b>	<b>0.258</b>	<b>0.038</b>	-0.118	0.350	-0.032	0.800
	Model2	0.244	0.061	0.111	0.397	-0.211	0.106	-0.075	0.571

Model 1 is non-adjusted

Model 2 is adjusted for maternal age, parity, GDM and gestational age, and fetal sex

## Discussion

Previous studies in the HAPO and other cohorts have demonstrated the effect of maternal obesity and gestational diabetes mellitus (GDM) on newborn size using metabolomic technology, suggesting that the intrauterine environment provided by mothers could affect newborn outcomes [24–26]. Our study group discovered that lower birth weight is an independent risk factor for later diabetes or IGT and showed for the first time that this risk factor also applies to a Chinese population [4], and both intrauterine under- and overnutritional status could affect insulin resistance in adulthood in animal experiments [27, 28], which was consistent with the developmental origins of health and disease (DoHAD) hypothesis. In this study, we aim to provide a new perspective from the view of newborns to discover the association of the metabolome between SGA, AGA, and LGA newborn babies and their mothers.

In this study, using an untargeted metabolomics approach, we show for the first time that specific metabolites were associated with both SGA and LGA mothers and their offspring, which might explain the phenomenon that children born with SGA and LGA had similar adverse outcomes. We observed that U-shaped metabolites were enriched in linoleic acid, arachidonic acid and glycerophospholipid metabolism. The metabolites associated with the

top 3 pathways were PC, citicoline and Prostaglandin E2. The importance of PC regulating lipid, lipoprotein and whole-body energy metabolism has been demonstrated in numerous dietary studies and knockout animal models [29]. For example, PC is an essential component of the very low-density lipoprotein (VLDL) complex [29], and the inhibition of hepatic PC synthesis impairs VLDL secretion and is linked to fatty liver disease in rodents as well as in human [30–32]. Related compounds of PC metabolic pathway, PC(14:0/22:5), PC(22:4/P-18:0), PG(16:1), and citicoline showed decreasing or increasing trends in both SGA/LGA maternal and fetal blood, which may indicate a disturbance of PC metabolism in these mother–offspring pairs.

In addition to pathway analysis, we screened 44 metabolites by p value, and identified that cuminaldehyde is lower in the SGA and LGA groups and is reported to be a volatile chemical constituent of cuminal seed [33]. It has been reported that cuminaldehyde presents in trace amounts in the blood and milk of ewes fed with cuminal seed [34], and its molecular weight is 148.205 Da, indicating that cuminaldehyde should be easily transported across the placental barrier. Cuminaldehyde was reported to have an inhibitory effect in vitro against rat lens aldose reductase and alpha-glucosidase (human metabolome database) and to protect against nonalcoholic fatty

liver disease in rats fed a high-fat diet [35]. This inhibitory action of cuminaldehyde suggests its potential utility as an antidiabetic therapeutic [36], and the potential mechanism might be associated with its insulinotropic and  $\beta$ -cell protective action [37]. In our study, cuminaldehyde was also significantly positively correlated with maternal adiponectin levels, negatively correlated with maternal BMI before pregnancy, and weight gain during pregnancy. These data indicate that cuminaldehyde is involved in lipid metabolism. According to previous reports, cuminaldehyde shows its superior activity for lipoxygenase (LOX) inhibitor, thereby blocking the oxidation of unsaturated fatty acids and inhibiting reactive oxygen species (ROS) production [33]. It is also quite interesting that adiponectin also showed a reverse effect against LOX-1 for reducing ROS production [38]. Therefore, due its anti-diabetic, anti-hepatotoxic and lipid metabolism modulating abilities, the low abundance of cuminaldehyde in both SGA/LGA maternal and neonatal blood might contribute to their increased metabolic risk.

2-Methoxy-estradiol-17 $\beta$  3-glucuronide was generated when UDP-glucuronate was transferred to UDP and was enriched in the SGA and LGA groups. Glucose is phosphorylated to glucose 6-phosphate in hepatocytes, which then produces UDP-glucose. UDP-glucose can be used to synthesize glycogen, UDP-glucuronate and UDP-galactose [39]. Even though the glucose in maternal and fetal blood showed no difference in the SGA, AGA and LGA groups in our study, the increased level of 2-methoxy-estradiol-17 $\beta$  3-glucuronide in the SGA/LGA groups might indicate a higher hepatic UDP-glucuronate transition rate in SGA and LGA newborns and their mothers. Recent research has also found that glucuronidation of bilirubin, drugs and xenobiotics in hepatocytes by glucuronide is considered a detoxification process [40]. Thus, the alteration in glucuronides concentrations might lead to impairment of the detoxification biological processes. Consistent with our hypothesis, abnormal glucuronide concentrations predict gestational diabetes in early pregnancy [41]. We also observed that the glucuronide was positively related with FFA in maternal blood, and negatively related with adiponectin in cord blood. Fatty acids have been reported to inhibit glucuronidation of different substrates [42, 43], which might explain the link of glucuronide to lipid index. These initial results are suggestive of a link between the abnormal abundance of certain metabolites in the intrauterine environment and the higher metabolic disorder development rate of both SGA and LGA newborns.

From the pathway analysis of line-shaped metabolites, we found out that top 3 pathways are all related to a series of phospholipids and fatty acids metabolites, including PC, PE, LysoPC and fatty acids. Since line-shaped metabolites are positively or negatively correlated

to newborn birthweight, we suppose that it might closely related to lipogenesis. The PC and PE are well studied for the role in lipid droplet formation [44, 45] and de novo lipogenesis regulation [46]. Therefore, it is plausible that the line-shaped metabolites are enriched in phospholipid metabolism pathways.

We also discover that serotonin, which was produced within the central nervous system and is in charge of regulating behavior, suppressing appetite and promoting energy expenditure, showed increasing trends [47]. Moreover, serotonin and insulin are colocalized in secretory beta-granules and are cosecreted by the stimulation of glucose [48]. Serotonin in adipose tissue promotes adipogenesis in white adipocytes, and elevated serotonin levels are associated with obesity. In our study, serotonin in maternal and fetal blood was also positively related to maternal BMI before pregnancy and the conventional biochemical index FFA, which indicated that the birthweight of newborns was possibly associated with maternal energy homeostasis.

13S-hydroxyoctadecadienoic acid, known as 13(S)-HODE, is the major lipoxygenation product synthesized in the body from linoleic acid and has been proposed as a biomarker for evaluating oxidative stress [49]. 13(S)-HODE has been reported to be increased in T2DM and alcohol-induced liver injury mouse models [50]. In our study, the level of 13(S)-HODE in maternal and cord blood showed increasing trends in the SGA, AGA and LGA groups and was significantly positively correlated with maternal prepregnancy BMI, weight gain, and HCY. Hyperhomocysteinemia is an independent risk factor for cardiovascular diseases and can also activate oxidative stress in endothelial cells [51]. Our results suggest that this oxidative stress marker, 13(S)-HODE, is positively correlated with neonatal birthweight, and related to maternal weight issues.

An additional interest in our study was the association of the maternal and fetal metabolome, which might explain the molecular mechanism underlying the DoHAD hypothesis of how the intrauterine environment regulates fetal metabolism. From the HAPO study [24], we can also tell that amino acids and acylcarnitine demonstrated significant correlations between maternal and cord blood levels via a series of transporters. Our analyses demonstrated that most of the metabolites in maternal blood showed a significant correlation with those in cord blood, including small molecule metabolites, such as the small polar molecules cuminaldehyde and serotonin, lipophilic molecule PG and 13(S)-HODE. Since most exchange across the placenta is driven by diffusion or specific transport proteins, small polar molecules and lipophilic substances dissolve readily through the entire syncytiotrophoblast plasma membrane and easily enter the fetal circulation system [18]. The same alterations

of maternal and fetal metabolome were also found in the preeclampsia pregnant groups, probably due to the metabolites passive transfer of metabolites across the placenta [52]. It has been reported that compounds, such as reactive oxygen species, which could reflect maternal metabolic status, may cross the placenta and affect the growing fetus in a similar fashion [53]. Therefore, some of the metabolites in cord blood are derived from transplacental transfer and are significantly influenced by maternal blood metabolite levels. Moreover, diffused metabolites could have a role in regulating fetal metabolism, which warrants further investigation. Despite differences in metabolomics, recent studies show that umbilical artery parameter is also correlated with newborn birthweight [54], especially in gestational diabetic mothers [55]. Therefore, we suppose that both maternal blood metabolites and umbilical artery hemodynamic factors influence birth weight.

This study had several strengths. An untargeted metabolomic assay was conducted to profile the whole picture of metabolites in both peripheral blood of pregnant women and cord blood of their babies, which could more extensively focus on molecular transfer in the intrauterine environment. We show for the first time that specific metabolites were associated with both SGA and LGA mothers and their offspring, which might explain why the children born with SGA and LGA had similar adverse outcomes. To further explore the clinical relevance of these metabolites, the correlation of maternal and fetal metabolomes with their phenotype was analyzed, and we found that maternal BMI, weight gain and adipokines, instead of blood glucose indices, were significantly associated with metabolite levels. The association of the maternal and fetal metabolome was also analyzed, and fetal metabolites in cord blood were significantly related to maternal blood metabolite levels. One limitation is that the confidence of metabolites annotation via non-targeted assays is limited, therefore the accurate quantification of our discovered metabolites need to be further confirmed by targeted assays and using standards for exact identification and quantitation. Another limitation is that the sample size of this study is relatively small. A larger cohort study with dietary records and animal models are planned to test these hypotheses.

In conclusion, we demonstrated a broad-scale association of metabolites between pregnant women and their offspring. We found 2 types of metabolites that changed with different patterns according to newborn birthweight. Among these metabolites, cuminaldehyde and glucuronide, denoted as “U-shaped” metabolites, associated with both the SGA and LGA groups have been reported to participate in glucose regulation, which might explain the phenomenon where these children

had similar adverse outcomes in adulthood. Serotonin and 13(S)-HODE are denoted as “line-shaped” metabolites, which correlate positively with newborn birthweight and are involved in energy homeostasis regulation and oxidative stress. These investigations demonstrate broad-scale metabolic differences related to newborn birthweight that help to provide new insights into insulin resistance and risks of metabolic syndrome in adults with SGA and LGA babies and might identify potential new markers for adverse newborn outcomes in pregnant women.

#### Abbreviations

SGA	Small-for-gestational
AGA	Appropriate-for-gestational
LGA	Large-for-gestational
BMI	Body mass index
MS	Mass spectrometers
PLS-DA	Partial least squares regression discriminant analysis
OPLS-DA	Orthogonal partial least squares regression discriminant analysis
VIP	Variable importance in projection
DMs	Differential metabolites

#### Supplementary Information

The online version contains supplementary material available at <https://doi.org/10.1186/s12884-023-05346-6>.

**Additional file 1: Figure S1.** OPLS-DA for negative mode.

**Additional file 2: Figure S2.** OPLS-DA for positive mode.

**Additional file 3: Figure S3.** Pathway analysis of (A) U-shaped metabolites and (B) line-shaped metabolites.

**Additional file 4: Table S1.** Characteristics of mothers and their offspring.

**Table S2.** Correlation of U-shape metabolites and blood index in cord blood. **Table S3.** Correlation of Line-shape metabolites and blood index in cord blood.

**Additional file 5: Table S4.** Metabolites and pathway information.

#### Acknowledgements

Not applicable.

#### Authors' contributions

X. X contributed to the study design, interpretation of findings and primary drafting of the manuscript. X.Z and J.L made equal contributions to all project components, including study design, acquisition of data and samples, metabolomic analysis, data analysis, interpretation of data, and manuscript drafting. M.Y, Q.Z and M.L contributed to study design and manuscript modification. N.Z contributed to data analysis, data interpretation and manuscript writing. J.L, Y.S, L.M, R.L, Z.Q, G.Z, and R.W contributed to study design and cord blood collection. X.X is the guarantor of this work and, as such, had full access to all the data in the study and take responsibility for the integrity of the data and the accuracy of the data analysis. The author(s) read and approved the final manuscript.

#### Funding

This study was funded by the grants from National Key Research and Development Program of China (2020YFC2004505), Chinese Academy of Medical Sciences Fundamental Research Funds for the Central Universities (3332018015), National High Level Hospital Clinical Research Funding (2022-PUMCH-C-019, 2022-PUMCH-C-023, and 2022-PUMCH-A-220), National Natural Science Foundation of China (No. 82170854, 81900723), and Beijing Natural Science Foundation (7202163).

## Availability of data and materials

The raw metabolomics data of the current study would be available from the corresponding author on reasonable request.

## Declarations

### Ethics approval and consent to participate

This study was approved by the Ethics Committee of the Peking Union Medical College Hospital and Xingtai People's Hospital (ZS-1484). All methods were performed in accordance with the relevant guidelines and regulations (Declaration of Helsinki). All participants have signed the Informed Consent.

### Consent for publication

Not Applicable.

### Competing interests

No potential conflicts of interest relevant to this article were reported.

### Author details

<sup>1</sup>Department of Endocrinology, Key Laboratory of Endocrinology, Ministry of Health, Peking Union Medical College Hospital, Chinese Academy of Medical Sciences & Peking Union Medical College, Beijing 100730, China. <sup>2</sup>Department of Medical Research Center, Peking Union Medical College Hospital, Chinese Academy of Medical Sciences & Peking Union Medical College, Beijing 100730, China. <sup>3</sup>Department of Obstetrics & Gynecology, Peking Union Medical College Hospital, Chinese Academy of Medical Sciences & Peking Union Medical College, Beijing 100730, China. <sup>4</sup>Department of Clinical Nutrition, Peking Union Medical College Hospital, Chinese Academy of Medical Sciences & Peking Union Medical College, Beijing 100730, China. <sup>5</sup>Department of Obstetrics & Gynecology, Xingtai People's Hospital, Xingtai, Hebei 054000, People's Republic of China.

Received: 6 April 2022 Accepted: 4 January 2023

Published online: 09 January 2023

## References

- Barker DJP. Sir Richard Doll Lecture. Developmental origins of chronic disease. *Public Health*. 2012;126(3):185–9.
- Hong YH, Lee JE. Large for gestational age and obesity-related comorbidities. *J Obes Metab Syndr*. 2021;30(2):124–31.
- Hong YH, Chung S. Small for gestational age and obesity related comorbidities. *Ann Pediatr Endocrinol Metab*. 2018;23(1):4–8.
- Xiao X, Zhang ZX, Cohen HJ, Wang H, Li W, Wang T, et al. Evidence of a relationship between infant birth weight and later diabetes and impaired glucose regulation in a Chinese population. *Diabetes Care*. 2008;31(3):483–7.
- Rueda-Clausen CF, Morton JS, Davidge ST. Effects of hypoxia-induced intrauterine growth restriction on cardiopulmonary structure and function during adulthood. *Cardiovasc Res*. 2009;81(4):713–22.
- Kramer MS, Zhang X, Dahhou M, Yang S, Martin RM, Oken E, et al. Does fetal growth restriction cause later obesity? Pitfalls in analyzing causal mediators as confounders. *Am J Epidemiol*. 2017;185(7):585–90.
- Fung C, Zinkhan E. Short- and long-term implications of small for gestational age. *Obstet Gynecol Clin North Am*. 2021;48(2):311–23.
- Eriksson JG, Forsen TJ, Osmond C, Barker DJ. Pathways of infant and childhood growth that lead to type 2 diabetes. *Diabetes Care*. 2003;26(11):3006–10.
- Pettitt DJ, Jovanovic L. Birth weight as a predictor of type 2 diabetes mellitus: the U-shaped curve. *Curr DiabRep*. 2001;1(1):78–81.
- Azadbakht L, Kelishadi R, Saraf-Bank S, Qorbani M, Ardalan G, Heshmat R, et al. The association of birth weight with cardiovascular risk factors and mental problems among Iranian school-aged children: the CASPIAN-III study. *Nutrition*. 2014;30(2):150–8.
- Lillicrop KA, Burdge GC. Epigenetic mechanisms linking early nutrition to long term health. *Best Pract Res Clin Endocrinol Metab*. 2012;26(5):667–76.
- Lumey LH, Khalangot MD, Vaiserman AM. Association between type 2 diabetes and prenatal exposure to the Ukraine famine of 1932–33: a retrospective cohort study. *Lancet Diabetes Endocrinol*. 2015;3(10):787–94.
- Li C, Lumey LH. Exposure to the Chinese famine of 1959–61 in early life and long-term health conditions: a systematic review and meta-analysis. *Int J Epidemiol*. 2017;46(4):1157–70.
- Fernandez-Twinn DS, Hjort L, Novakovic B, Ozanne SE, Saffery R. Intrauterine programming of obesity and type 2 diabetes. *Diabetologia*. 2019;62(10):1789–801.
- Viswanathan S, McNelis K, Makker K, Calhoun D, Woo JG, Balagopal B. Childhood obesity and adverse cardiometabolic risk in large for gestational age infants and potential early preventive strategies: a narrative review. *Pediatr Res*. 2021;92(3):653–61.
- Godfrey KM, Reynolds RM, Prescott SL, Nyirenda M, Jaddoe VW, Eriksson JG, et al. Influence of maternal obesity on the long-term health of offspring. *Lancet Diabetes Endocrinol*. 2017;5(1):53–64.
- Franks PW, Looker HC, Kobes S, Touger L, Tataranni PA, Hanson RL, et al. Gestational glucose tolerance and risk of type 2 diabetes in young Pima Indian offspring. *Diabetes*. 2006;55(2):460–5.
- Desforges M, Sibley CP. Placental nutrient supply and fetal growth. *Int J Dev Biol*. 2010;54(2–3):377–90.
- Dunn WB, Broadhurst D, Begley P, Zelena E, Francis-McIntyre S, Anderson N, et al. Procedures for large-scale metabolic profiling of serum and plasma using gas chromatography and liquid chromatography coupled to mass spectrometry. *Nat Protoc*. 2011;6(7):1060–83.
- Zhu L, Zhang R, Zhang S, Shi W, Yan W, Wang X, et al. Chinese neonatal birth weight curve for different gestational age. *Zhonghua Er Ke Za Zhi*. 2015;53(2):97–103.
- Kanehisa M, Goto S. KEGG: kyoto encyclopedia of genes and genomes. *Nucleic Acids Res*. 2000;28(1):27–30.
- Lu L, Koulman A, Petry CJ, Jenkins B, Matthews L, Hughes IA, et al. An unbiased lipidomics approach identifies early second trimester lipids predictive of maternal glycemic traits and gestational diabetes mellitus. *Diabetes Care*. 2016;39(12):2232–9.
- Pang Z, Chong J, Zhou G, de Lima Morais DA, Chang L, Barrette M, et al. MetaboAnalyst 5.0: narrowing the gap between raw spectra and functional insights. *Nucleic acids research*. 2021;49(W1):W388–w96.
- Lowe WL Jr, Bain JR, Nodzenski M, Reisetter AC, Muehlbauer MJ, Stevens RD, et al. Maternal BMI and Glycemia impact the fetal metabolome. *Diabetes Care*. 2017;40(7):902–10.
- Scholtens DM, Muehlbauer MJ, Daya NR, Stevens RD, Dyer AR, Lowe LP, et al. Metabolomics reveals broad-scale metabolic perturbations in hyperglycemic mothers during pregnancy. *Diabetes Care*. 2014;37(1):158–66.
- Scholtens DM, Bain JR, Reisetter AC, Muehlbauer MJ, Nodzenski M, Stevens RD, et al. Metabolic networks and metabolites underlie associations between maternal glucose during pregnancy and newborn size at birth. *Diabetes*. 2016;65(7):2039–50.
- Zheng J, Xiao X, Zhang Q, Yu M, Xu J, Wang Z. Maternal protein restriction induces early-onset glucose intolerance and alters hepatic genes expression in the peroxisome proliferator-activated receptor pathway in offspring. *J Diabetes Investig*. 2015;6(3):269–79.
- Zheng J, Xiao X, Zhang Q, Yu M, Xu J, Wang Z. Maternal high-fat diet modulates hepatic glucose, lipid homeostasis and gene expression in the PPAR pathway in the early life of offspring. *Int J Mol Sci*. 2014;15(9):14967–83.
- van der Veen JN, Kennelly JP, Wan S, Vance JE, Vance DE, Jacobs RL. The critical role of phosphatidylcholine and phosphatidylethanolamine metabolism in health and disease. *Biochim Biophys Acta Biomembr*. 2017;1859(9 Pt B):1558–72.
- Li Z, Agellon LB, Allen TM, Umeda M, Jewell L, Mason A, et al. The ratio of phosphatidylcholine to phosphatidylethanolamine influences membrane integrity and steatohepatitis. *Cell Metab*. 2006;3(5):321–31.
- Walkey CJ, Yu L, Agellon LB, Vance DE. Biochemical and evolutionary significance of phospholipid methylation. *J Biol Chem*. 1998;273(42):27043–6.
- Ling J, Chaba T, Zhu LF, Jacobs RL, Vance DE. Hepatic ratio of phosphatidylcholine to phosphatidylethanolamine predicts survival after partial hepatectomy in mice. *Hepatology (Baltimore, MD)*. 2012;55(4):1094–102.
- Tomy MJ, Dileep KV, Prasanth S, Preethidan DS, Sabu A, Sadasivan C, et al. Cuminaldehyde as a lipoxygenase inhibitor: in vitro and in silico validation. *Appl Biochem Biotechnol*. 2014;174(1):388–97.

34. Désage M, Schaal B, Soubeyrand J, Orgeur P, Brazier JL. Gas chromatographic-mass spectrometric method to characterise the transfer of dietary odorous compounds into plasma and milk. *J Chromatogr B Biomed Appl*. 1996;678(2):205–10.
35. Haque MR, Ansari SH. Aromatic aldehyde compound cuminaldehyde protects nonalcoholic fatty liver disease in rats feeding high fat diet. *Hum Exp Toxicol*. 2019;38(7):823–32.
36. Lee HS. Cuminaldehyde: Aldose reductase and alpha-glucosidase inhibitor derived from *Cuminum cyminum* L. Seeds. *J Agric Food Chem*. 2005;53(7):2446–50.
37. Patil SB, Takalikar SS, Joglekar MM, Haldavnekar VS, Arvindekar AU. Insulinotropic and  $\beta$ -cell protective action of cuminaldehyde, cuminol and an inhibitor isolated from *Cuminum cyminum* in streptozotocin-induced diabetic rats. *Br J Nutr*. 2013;110(8):1434–43.
38. Chen X, Zhang H, McAfee S, Zhang C. The reciprocal relationship between adiponectin and LOX-1 in the regulation of endothelial dysfunction in ApoE knockout mice. *Am J Physiol Heart Circ Physiol*. 2010;299(3):H605–12.
39. Adeva-Andany MM, Pérez-Felpete N, Fernández-Fernández C, Donapetry-García C, Pazos-García C. Liver glucose metabolism in humans. *Biosci Rep*. 2016;36(6):e00416.
40. Yang G, Ge S, Singh R, Basu S, Shatzer K, Zen M, et al. Glucuronidation: driving factors and their impact on glucuronide disposition. *Drug Metab Rev*. 2017;49(2):105–38.
41. Koos BJ, Gornbein JA. Early pregnancy metabolites predict gestational diabetes mellitus: implications for fetal programming. *American journal of obstetrics and gynecology*. 2021;224(2):215.e1–e7.
42. Zhong Z, Kauffman FC, Thurman RG. Inhibition of glucuronidation of benzo(a)pyrene phenols by long-chain fatty acids. *Can Res*. 1991;51(17):4511–5.
43. Rowland A, Knights KM, Mackenzie PI, Miners JO. The “albumin effect” and drug glucuronidation: bovine serum albumin and fatty acid-free human serum albumin enhance the glucuronidation of UDP-glucuronosyltransferase (UGT) 1A9 substrates but not UGT1A1 and UGT1A6 activities. *Drug Metab Dispos*. 2008;36(6):1056–62.
44. Guo Y, Walther TC, Rao M, Stuurman N, Goshima G, Terayama K, et al. Functional genomic screen reveals genes involved in lipid-droplet formation and utilization. *Nature*. 2008;453(7195):657–61.
45. Krahmer N, Guo Y, Wilfling F, Hilger M, Lingrell S, Heger K, et al. Phosphatidylcholine synthesis for lipid droplet expansion is mediated by localized activation of CTP:phosphocholine cytidyltransferase. *Cell Metab*. 2011;14(4):504–15.
46. Lim HY, Wang W, Wessells RJ, Ocorr K, Bodmer R. Phospholipid homeostasis regulates lipid metabolism and cardiac function through SREBP signaling in *Drosophila*. *Genes Dev*. 2011;25(2):189–200.
47. Yabut JM, Crane JD, Green AE, Keating DJ, Khan WI, Steinberg GR. Emerging roles for serotonin in regulating metabolism: new implications for an ancient molecule. *Endocr Rev*. 2019;40(4):1092–107.
48. Sun EWL, Martin AM, Young RL, Keating DJ. The Regulation of peripheral metabolism by gut-derived hormones. *Front Endocrinol*. 2018;9:754.
49. Murotomi K, Umeno A, Yasunaga M, Shichiri M, Ishida N, Abe H, et al. Switching from singlet-oxygen-mediated oxidation to free-radical-mediated oxidation in the pathogenesis of type 2 diabetes in model mouse. *Free Radical Res*. 2015;49(2):133–8.
50. Zhang W, Zhong W, Sun Q, Sun X, Zhou Z. Hepatic overproduction of 13-HODE due to ALOX15 upregulation contributes to alcohol-induced liver injury in mice. *Sci Rep*. 2017;7(1):8976.
51. Au-Yeung KK, Woo CW, Sung FL, Yip JC, Siow YL, O K. Hyperhomocysteinemia activates nuclear factor- $\kappa$ B in endothelial cells via oxidative stress. *Circulation Res*. 2004;94(1):28–36.
52. Youssef L, Simões RV, Miranda J, García-Martín ML, Paules C, Crovetto F, et al. Paired maternal and fetal metabolomics reveal a differential fingerprint in preeclampsia versus fetal growth restriction. *Sci Rep*. 2021;11(1):14422.
53. Youssef L, Erlandsson L, Åkerström B, Miranda J, Paules C, Crovetto F, et al. Hemopexin and  $\alpha$ 1-microglobulin heme scavengers with differential involvement in preeclampsia and fetal growth restriction. *PLoS ONE*. 2020;15(9):e0239030.
54. Sirico A, Diemert A, Glosemeyer P, et al. Third trimester umbilical artery doppler in low-risk pregnancies and its correlation to estimated fetal weight and birthweight. *Ultraschall Med*. 2021;42(3):285–90.
55. Sirico A, Rizzo G, Maruotti GM, et al. Does fetal macrosomia affect umbilical artery Doppler velocity waveforms in pregnancies complicated by gestational diabetes? *J Matern Fetal Neonatal Med*. 2016;29(20):3266–70.

## Publisher's Note

Springer Nature remains neutral with regard to jurisdictional claims in published maps and institutional affiliations.

**Ready to submit your research? Choose BMC and benefit from:**

- fast, convenient online submission
- thorough peer review by experienced researchers in your field
- rapid publication on acceptance
- support for research data, including large and complex data types
- gold Open Access which fosters wider collaboration and increased citations
- maximum visibility for your research: over 100M website views per year

**At BMC, research is always in progress.**

Learn more [biomedcentral.com/submissions](https://biomedcentral.com/submissions)

